



Published in final edited form as:

Mol Cancer Ther. 2013 December ; 12(12): . doi:10.1158/1535-7163.MCT-12-0719.

Selective disruption of Rb-Raf-1 kinase interaction inhibits pancreatic adenocarcinoma growth irrespective of gemcitabine sensitivity

José G. Treviño^{1,4}, Monika Verma^{1,#}, Sandeep Singh^{1,\$}, Smitha Pillai¹, Dongyu Zhang⁴, Daniele Pernazza², Said M. Sebti², Nicholas J. Lawrence², Barbara A. Centeno³, and Srikumar P. Chellappan^{1,*}

¹Dept. of Tumor Biology

²Dept. of Drug Discovery

³Dept. of Anatomic Pathology H. Lee Moffitt Cancer Center & Research Institute, 12902 Magnolia Drive, Tampa, FL 33612.

⁴Dept. of Surgery University of Florida-Gainesville, 1600 SW Archer Rd, Gainesville, FL 32610

Abstract

Inactivation of the Retinoblastoma tumor suppressor protein, (Rb), is widespread in human cancers. Inactivation of Rb is thought to be initiated by association with Raf-1 (C-Raf) kinase, and here we determined how RRD-251, a disruptor of the Rb-Raf-1 interaction, affects pancreatic tumor progression. Assessment of phospho-Rb levels in resected human pancreatic tumor specimens by immunohistochemistry ($n=95$) showed that increased Rb phosphorylation correlated with increasing grade of resected human pancreatic adenocarcinomas ($p=0.0272$), which correlated with reduced overall patient survival ($p=0.0186$). To define the anti-tumor effects of RRD-251 (50 μ M), cell-cycle analyses, senescence, cell viability, cell migration, anchorage-independent growth, angiogenic tubule formation and invasion assays were performed on gemcitabine sensitive and resistant pancreatic cancer cells. RRD-251 prevented S-phase entry, induced senescence and apoptosis, and inhibited anchorage-independent growth and invasion ($p<0.01$). Drug efficacy on subcutaneous and orthotopic xenograft models was tested by intraperitoneal injections of RRD-251 (50mpk) alone or in combination with gemcitabine (250mg/kg). RRD-251 significantly reduced tumor growth *in vivo* accompanied by reduced Rb phosphorylation and lymph node and liver metastasis ($p<0.01$). Combination of RRD-251 with gemcitabine demonstrated cooperative effect on tumor growth ($p<0.01$). In conclusion, disruption of the Rb-Raf-1 interaction significantly reduces the malignant properties of pancreatic cancer cells irrespective of their gemcitabine sensitivity. Selective targeting of Rb-Raf-1 interaction might be a promising strategy targeting pancreatic cancer.

Keywords

Pancreatic cancer; Retinoblastoma tumor suppressor protein; Rb; Raf-1 kinase; RRD-251

*Corresponding author: Phone: (813) 745-6892 Fax: (813) 745-6748 Srikumar.Chellappan@moffitt.org.

#Current address: University of Michigan, Ann Arbor, Michigan

\$National Institute of Biomedical Genomics, Kalyani, West Bengal, India.

The authors have no conflicts of interest to declare.

Introduction

Pancreatic adenocarcinoma remains the fourth leading cause of cancer-related deaths (1). Even after potential curative surgery and adjuvant therapies, the overall 5-year survival rate remains approximately 5% (2). Additionally, chemotherapy with gemcitabine alone provides poor long-term outcome, with the possible acquisition of gemcitabine resistance by a variety of molecular aberrations that have not been fully defined (3, 4). Therefore, further understanding the molecular mechanisms involved in the genesis, progression, chemoresistance, and metastasis of pancreatic cancers might lead to the development of more effective therapeutic strategies.

The retinoblastoma tumor suppressor protein, Rb, is the major regulator of the mammalian cell-cycle progression (5-7). Rb prevents cell-cycle progression by physically interacting with E2F family of transcription factors repressing their transcriptional activity (8). Phosphorylation of Rb protein by cyclin dependent kinases, mainly Cdk2, Cdk4 and Cdk6, leads to the dissociation of E2Fs from Rb, enabling them to induce downstream target genes that are necessary for cell-cycle progression (7). Thus, agents that can prevent Rb phosphorylation and maintain its functional state can be expected to have a cytostatic effect with subsequent anti-tumor activities (5). Although Rb phosphorylation is mediated mainly by cyclin-dependent kinases, Raf-1 could bind and phosphorylate Rb early in the cell-cycle, facilitating subsequent phosphorylation and complete inactivation (5, 9). An eight amino-acid peptide inhibiting Rb-Raf-1 interactions confirmed this hypothesis (10) and development of a small molecule inhibitor of the Rb-Raf-1 interaction, RRD-251, prevented Rb phosphorylation and subsequent growth of lung cancer and melanoma (7, 11). In invasive pancreatic adenocarcinoma, Rb expression correlates with histological grade and nodal involvement (12, 13) therefore promoting investigations toward therapies against Rb phosphorylation.

Here we demonstrate that Rb phosphorylation correlates with more advanced disease in human pancreatic tumor tissues which correlates with poor overall survival. Inhibition of Rb phosphorylation with RRD-251 led to an inhibition of proliferation, migration, and invasion in a pancreatic cancer cell lines, including highly metastatic cells that are resistant to gemcitabine. RRD-251 also prevented the *in vivo* growth and metastasis of pancreatic cancer cells xenograft models. Importantly, the combination therapy of gemcitabine and RRD-251 demonstrated chemotherapeutic sensitization in xenograft models. These results suggest that targeting the Rb-Raf-1 interaction might be a potential avenue to combat pancreatic cancer.

Materials & Methods

Cell lines and reagents

PANC-1 and Mia-PaCa-2 human pancreatic cancer cells were obtained from American Type Culture Collection (Rockville, MD) and were used within six months; they have been re-authenticated by STR analysis. The L3.6pl metastatic variant pancreatic cancer cell line was derived as previously described (14, 15). The cells were maintained in culture in Dulbecco's Modified Eagle Medium supplemented with 10% fetal bovine serum (Hyclone, Logan, UT), and 0.6% penicillin/streptomycin/amphotericin-B (Hyclone). RRD-251 was suspended in DMSO as previously described (11). Gemcitabine (Eli Lilly) was suspended in Dulbecco's phosphate-buffered saline (D-PBS).

Selection of L3.6pl^{GemRes} gemcitabine-resistant pancreatic cancer cells

Selection of L3.6pl^{GemRes} gemcitabine-resistant pancreatic cancer cells was performed as previously described (16). L3.6pl gemcitabine-sensitive cells were exposed to 5 μ M of

gemcitabine. The dose was steadily increased by 5 μ M increments every two days to maximal concentration of 30 μ M, approximately 12-fold greater than the IC₅₀. Single colonies of gemcitabine-resistant clones were isolated and expanded for further analysis. Persistence of gemcitabine resistance was confirmed by maintenance of cells without gemcitabine for 6-weeks followed by return to maintenance gemcitabine concentrations (5 μ M) with no effect on cellular proliferation or apoptosis. Authentication of this cell line showed that its short tandem repeat profile is identical to the parental cell line, L3.6pl.

Lysate preparation, immunoprecipitation, and western blotting

Lysates were prepared from cells and tumor tissues as previously described (11). Physical interaction between Rb-Raf-1 and Rb-E2F1 was analyzed by immunoprecipitating Raf-1 and E2F1 as previously described (10). Monoclonal Rb and Raf-1 antibodies (BD Transduction Laboratories) and E2F1 (Santa Cruz Biotechnology), polyclonal phosphorylated Rb and PARP antibodies (Cell Signaling Technology), Mcl-1, Bcl-2, and Bax antibodies (Santa Cruz Biotechnology), β -actin (Sigma-Aldrich) were used for western blot analyses.

Cell-cycle and apoptotic analysis by flow cytometric analyses

Cells were serum starved for 48 hours and subsequently serum-stimulated in the presence or absence of RRD-251 for 18 hours. Cells were washed in D-PBS, harvested, centrifuged, and pellet re-suspended in 0.1 ml of citrate/DMSO buffer. Samples were processed per Vindelov method and cell cycle analysis was performed by flow cytometry (7, 17). For detection of apoptosis, cells were treated with RRD-251 for 24 hours and apoptosis was detected by 7-AAD and Annexin V staining (BD Pharmingen) as previously described(18).

Cell viability/cytotoxicity and senescence assays

Cell viability was quantified by MTT assay (Trivegen). Cells were allowed to adhere overnight. Cells were treated with RRD-251 (10-100 μ M) or DMSO in complete media and viability assayed after 48 hours using published protocols (19). Senescence was determined after treatment with RRD-251 (50 μ M), cdk inhibitor PD0332991 (2.5 μ M) (Selleck Chemical) or vehicle control (DMSO) for 48 hrs. The cells were stained with β -galactosidase per senescence staining kit protocols (Cell Signaling). The blue senescent cells were quantified by counting four different fields (20X).

Soft agar colony formation assay

5,000 cells were suspended in 0.3% agarose and layered on top of 0.6% bottom agarose in twelve well sterile plates (Corning). Plates were covered with 1ml of complete medium with 50 μ M RRD-251 (in DMSO) or DMSO and incubated for 3 weeks. RRD-251 was refreshed twice weekly in complete media. The colonies were stained with MTT as previously described (7).

Wound healing and invasion assays

Cells grown to 90% confluency were scratched at three different areas. Cells were treated with RRD-251 (50 μ M) or DMSO control for 18 hours, and. multiple images were taken before and after treatment. For invasion assays, cells were pre-treated with 50 μ M RRD-251 for 4 hours and 20,000 cells were plated in the upper chamber of the filter in 10% FBS and 0.1% bovine serum albumin containing media (Sigma). Media containing 20% fetal bovine serum was placed in the lower well as an attractant. After 18-hours, the filters were fixed in methanol and stained with hematoxylin. Invading cells were imaged and quantified by counting four different fields.

Angiogenic tubule formation assay

Matrigel (Collaborative Biomedical Products) was used to assess the differentiation of human umbilical vascular endothelial cells (HUVEC) into capillary tube-like structures (10). Matrigel was added to 96-well tissue culture plates, followed by incubation at 37°C for 60 minutes to allow polymerization. Subsequently, 1×10^4 HUVECs were seeded in EGM2 medium (Clonetics) supplemented with 5% FBS in the presence or absence of 20, 50, and 100 $\mu\text{mol/L}$ concentrations of RRD-251 and incubated for 18h at 37°C. Capillary tube formation was assessed using a Leica DMIL phase contrast microscope.

Real-time PCR

HUVECs were serum-starved for 24-hours, pretreated with RRD-251 at indicated doses, and subsequently stimulated with VEGF (100ng/ml). Total RNA was isolated using the RNeasy kit (Qiagen, CA). Levels of FLT-1 and KDR mRNA were analyzed by quantitative reverse transcription PCR. The primers used for amplifying FLT1 mRNA were FLT-1 F5' AGCGATTGCATTGACCTG and FLT-1 R5' GGTACGAATCGACCGAATC and for KDR mRNA the primers used were KDR F5' CATTGACCTGCCGAAT, KDR R 5'CCGAATCCTAAGACTG. Data were normalized using 18S rRNA as internal control and the fold change in the expression levels was determined as described (20).

Mouse xenograft experiments

For subcutaneous implantation, 1×10^6 pancreatic cancer cells were implanted in the subcutaneous flank tissue of 8-week old female athymic nude mice (Charles River Laboratories) using a minimum of 6 mice per group. After the tumor growth was established (100mm³), RRD-251 was administered intraperitoneally daily at 50 mg per kilograms (mpk) in DMSO vehicle. For gemcitabine treatment, IP dosing of gemcitabine at 250mg/kg was scheduled every alternate day (three times/week). Tumor volumes were determined three times a week by measuring length (L) and width (W), and calculating volume ($V = 1/2 \times L \times W^2$). Mice were euthanized at 14-16 days and tumors harvested for further analysis. For orthotopic implantation, a left abdominal flank incision was performed with exteriorization of the spleen and pancreas, and 2.5×10^5 cells were injected into the subcapsular region of the body of the pancreas as previously described (19). One week after injections, mice were treated with RRD-251 or DMSO control daily. Mice were euthanized 4 weeks after implantation and primary tumors, regional peri-pancreatic (celiac and para-aortic) lymph nodes, and livers were harvested for further analyses. All animal experiments were conducted with approval from the institutional IACUC.

Pancreatic cancer tissue microarrays

All cases of resected pancreatic ductal adenocarcinoma (PDAC) used to generate tissue microarrays (TMAs) were resected at the H. Lee Moffitt Cancer Center and Research Institute from 1987 to 2006; these studies were conducted under a protocol approved by the USF IRB. Two separate cores, 0.6 cm in diameter, were obtained for each area of carcinoma as well as from the nonmalignant areas. Sections of the TMA were stained with H&E using standard techniques (19). The TMAs were reviewed and grade (I-IV) assigned to the each core containing carcinoma using a standard grading system.

Immunohistochemistry

Immunohistochemical staining was performed using a Ventana Discovery XT automated system (Tucson, AZ) as per manufacturer's protocol with proprietary reagents (21). Primary antibody against phospho-Rb, (Cell Signaling) and CD31 antibody (Abcam, Cambridge, MA) was used for IHC. Stained slides were scanned on an Ariol SL-50 Automatic Scanning System. Both the intensity and percentage of cells expressing phospho-Rb were assessed.

The intensity of nuclear staining was assessed as 0 (absent), 1+(weak), 2+(moderate) and 3+ (strong) for pRb. Each core was assigned a histoscore consisting of the sum of the product of each intensity and the percentage of cells positive at that intensity (histoscore= $(0 \times 0) + 1 \times \% \text{ cells} + 2 \times \% \text{ cells} + (3 \times \% \text{ cells}) + (4 \times \% \text{ cells})$).

Statistical analyses

Statistical analysis was performed using two-tailed Student's *t*-test. Experiments were performed in triplicate and values were considered significant when the *p*-value was <0.05 . Tissue microarray immunohistochemical analyses are expressed as the mean \pm standard deviation. Correlation between staining extent and intensity was determined by Spearman's correlation coefficient. One-way ANOVA was used to correlate pRB score with grade. Disease-specific survival was estimated by the Kaplan-Meier method.

Results

Rb phosphorylation correlates with tumor grade/differentiation in human pancreatic tumor specimens

To determine if Rb phosphorylation correlates with tumor grade pancreatic cancer tissue microarrays were stained for phospho-Rb. Assessment of grade within each core showed the following distribution: nine grade I carcinomas (well-differentiated), 55 grade II carcinomas (moderately-differentiated), 31 grade III carcinomas (including one adenosquamous carcinoma shown in poorly-differentiated, Figure 1A, upper panel) and 1 grade IV carcinoma. All grades showed intensity ranging from 0-3 and a pRb-staining product (score) ranging from 0-300. The mean pRb score for each grade is as follows: 107.8 for grade I (107.8 ± 59.1), 131.1 for grade II (131.1 ± 86.6) and 177.4 for grade III and IV combined (177.4 ± 82.7). Comparison of phospho-Rb levels with grade of PDAC stratified into two categories (low grade= grades I and II, high grade = grades III and IV) showed a statistically significant difference in expression ($p=0.0272$) (Figure 1A, lower panel), with increased Rb phosphorylation correlating with higher grade. Overall survival correlated with grade using our two-tiered classification ($p=0.0186$). Thus, high-grade PDAC, which correlates with poorer survival, are tumors that have more phosphorylated Rb; future studies on larger cohorts of patients will be needed to confirm these correlations.

Disruption of Rb-Raf-1 interaction inhibits anchorage-independent growth

Since clinical samples suggested a correlation of Rb phosphorylation with reduced differentiation, we examined whether RRD-251 affected Rb phosphorylation. Western blots conducted on L3.6pl, L3.6pl^{GemRes}, PANC-1 and Mia-PaCa-2 cells treated with 50 μ M RRD-251 for 24 hours showed a reduction in the slower migrating hyper-phosphorylated form of Rb (Figure 1B, upper panel). To examine whether this correlated with a disruption of Rb-Raf-1 binding, cells were serum-starved for 48-hours and serum-stimulated for two hours in the presence or absence of RRD-251. Immunoprecipitation-western blot analysis showed that RRD-251 treatment led to a significant reduction in the serum-induced binding of Raf-1 to Rb (Figure 1B, lower panel). RRD-251 did not disrupt the binding of E2F1 to Rb (Figure 1C), as we had seen in other cell lines. We next examined the effects of RRD-251 on the adherence-independent growth of PANC-1, Mia-PaCa-2, and L3.6pl metastatic variants. RRD-251 significantly inhibited anchorage-independent growth of cells in soft agar (Figure 1D). Structure of RRD-251 is shown in Figure 1E. These results suggest that RRD-251 can disrupt Rb-Raf-1 binding and Rb-phosphorylation and significantly inhibit anchorage-independent growth of cell lines.

Disruption of Rb-Raf-1 interaction results in inhibition of proliferation and induction of senescence

Previous studies demonstrated that RRD-251 induces G1 arrest in lung cancer cells but induces apoptosis in melanoma cells (7). To determine how RRD-251 affects pancreatic cancer cells, PANC-1 and Mia-PaCa-2, metastatic variant L3.6pl, and L3.6pl^{GemRes} cells were treated with 50 μ M RRD-251 for 48-hours. Western blot analysis showed cleavage of PARP indicative of apoptosis, in both PANC-1 and Mia-PaCa-2 cells; there was no significant apoptosis in the metastatic cell lines (Figure 2A, upper panel). RRD-251 treatment of L3.6pl, MIA-PaCa-2, and PANC-1 cells and showed a decrease in levels of anti-apoptotic proteins Bcl-2 and Mcl-1 and increased the pro-apoptotic protein Bax (Figure 2A, lower panel). Further, determination of apoptosis by Annexin V by flow cytometry determined that RRD-251 could result in significant induction of apoptosis in PANC-1 (33.4% early and 50.8% late apoptosis) and MIA-PaCa-2 (10.4% early and 14.1% late apoptosis), but no significant change in L3.6pl and L3.6pl^{GemRes} cells when compared to controls (Supplementary Figures 1 and 2 and Supplementary Tables 1 and 2). Since metastatic L3.6pl cells were resistant to RRD-251-induced apoptosis, further experiments were conducted to assess how RRD-251 inhibited the growth of L3.6pl and L3.6pl^{GemRes} cells. L3.6pl and L3.6pl^{GemRes} were exposed to different concentrations of RRD-251 (10-100 μ M) and cell viability was quantified after 48-hours. Viability of L3.6pl cells was significantly reduced in a dose-dependent manner ($p < 0.01$, Figure 2B) whereas L3.6pl^{GemRes} cells was affected to a lesser extent. Since RRD-251 did not induce apoptosis in these cells, we examined whether the inhibitory effects could be due to an arrest in cell-cycle progression (7). As shown in Figure 2C, there was a 65% reduction in S-phase and 50% increase in G1 phase in L3.6pl cell populations treated with RRD-251 (left panels), and a 61% reduction in S-phase and 54% increase in G1 phase in L3.6pl^{GemRes} cells (Figure 2C, right panels). Attempts were also made to assess whether the cell cycle arrest also coincided with induction of cellular senescence. To further elucidate the mechanism of RRD-251, staining for senescence-associated β -galactosidase showed that RRD-251 significantly induced cellular senescence (Figure 2D) to r levels induced by CDK inhibitor PD0332991, a known inducer of senescence (22, 23). These results suggest that RRD-251 induces both cell cycle arrest and cellular senescence in metastatic and gemcitabine resistant pancreatic cancer cells.

RRD-251 enhances the effects of gemcitabine to promote apoptosis and inhibit anchorage independent growth in gemcitabine-resistant L3.6pl^{GemRes}

To determine the effect of combination therapy of RRD-251 with gemcitabine (Figure 3A), acquired gemcitabine resistance was confirmed by continued growth and resistance to PARP cleavage of L3.6pl^{GemRes} cells in the presence of gemcitabine when compared to parental L3.6pl (Figure 3B). Since RRD-251 did not induce apoptosis in the metastatic variant L3.6pl or L3.6pl^{GemRes}, we examined whether combining RRD-251 with gemcitabine had an effect. Towards this purpose, L3.6pl^{GemRes} cells were exposed to gemcitabine (5 μ M), RRD-251 (50 μ M), or in combination. While gemcitabine resulted in a 70% decrease in viability of the L3.6pl parental cell line, RRD-251 alone or in combination with gemcitabine demonstrated a 61% and 87% decrease in viability respectively, suggesting a sensitization to combination therapy. Additionally, while gemcitabine alone did not have an inhibitory effect in the L3.6pl^{GemRes}, but rather a 1.3-fold increase in cell viability, RRD-251 alone resulted in a 50% reduction in its viability. Combination of RRD-251 with gemcitabine further inhibited the viability by 69% (Figure 3C), suggesting an enhanced effect with combination therapy on gemcitabine-resistant cells. To examine whether this reduction in viability was due to apoptosis, PARP cleavage was examined by western blotting. Gemcitabine or RRD-251 alone did not induce PARP cleavage or changes in apoptotic proteins in L3.6pl^{GemRes} cells, but treatment with combination of RRD-251 and gemcitabine resulted in

PARP cleavage; this correlated with decreased expression of anti-apoptotic proteins Bcl-2 and Mcl-1, an increase in pro-apoptotic protein Bax (Figure 3D, upper panel). To confirm our PARP cleavage results, we performed Annexin V staining flow cytometry on L3.6pl and L3.6pl^{GemRes} pancreatic cancer cells treated with gemcitabine, RRD-251, or in combination. Our results demonstrate only combination treatment with RRD-251 and gemcitabine significantly induced apoptosis (19.8% early and 45.5% late apoptosis) in L3.6pl^{GemRes} gemcitabine resistant cells (Supplementary Figure 2 and Supplementary Table 2). Although experiments with RRD-251 alone demonstrated a significant reduction in anchorage-independent growth in L3.6pl cells, a less robust effect was observed in L3.6pl^{GemRes} cells; but combination of RRD-251 and gemcitabine demonstrated almost complete abrogation of growth (Figure 3D, lower panel). Overall, these results suggest the inhibitory effects on RRD-251 alone were likely due to cell-cycle arrest in the metastatic pancreatic cancer cell lines, but combination with gemcitabine induced apoptosis in gemcitabine resistant L3.6pl^{GemRes} cells.

Rb-Raf-1 kinase disruption inhibits migration, invasion, and angiogenic potential

Wound-healing assays were conducted to determine whether RRD-251 alone or in combination with gemcitabine affects migration of L3.6pl and L3.6pl^{GemRes} cells. While gemcitabine significantly inhibited the ability of L3.6pl cell to migrate, the L3.6pl^{GemRes} continued to migrate in the presence of gemcitabine. RRD-251 alone or combination with gemcitabine significantly reduced the migratory capacity of both populations (Figure 3E). As shown in Figure 3F, while gemcitabine marginally increased invasion in the L3.6pl^{GemRes} cells, RRD-251 alone resulted in a 74% reduction in the invasion of both L3.6pl and L3.6pl^{GemRes} cells. Combination of RRD-251 with gemcitabine resulted in 96% and 91% reduction in the invasive capacity of L3.6pl and L3.6pl^{GemRes} cells respectively ($p < 0.001$, Figure 3F). Additionally, treatment with RRD-251 led to a marked inhibition of angiogenic tubule formation (Figure 4A, left panel). Previously, we had observed that VEGF, FLT-1 and KDR receptors have E2F binding sites, which respond to the Rb-E2F pathway (20). In our studies, it was found that RRD-251 significantly inhibited the expression of FLT-1 and KDR, potentially leading to the inhibition of angiogenic tubule formation (Figure 4A, right panel). It appears that RRD-251 can not only affect the viability of pancreatic cancer cells, but also affect processes like migration, invasion and angiogenesis, which facilitate the progression and metastasis of pancreatic cancers.

RRD-251 inhibits primary tumor growth in subcutaneous and orthotopic xenograft models and significantly affects metastatic potential *in vivo*

We next determined the effects of RRD-251 on pancreatic cancer cells *in vivo* utilizing subcutaneous and orthotopic xenograft models. L3.6pl cells were implanted bilaterally on the flanks of athymic nude mice in the subcutaneous model; 50mpk of RRD-251 or vehicle was administered intraperitoneally daily after the implanted tumors reached 100mm³ size. After 14 days of treatment, tumor growth in the RRD-251 group (117±20mm³) was significantly lower compared to vehicle control (1094±67mm³, $p < 0.001$, Figure 4B). This difference in tumor size was confirmed by measurements *ex vivo* (Figure 4B, inset). IP-WB analysis of resected tumors showed a significant reduction in Rb bound to Raf-1 in the RRD-251 treated mice (Figure 4B, left panel). Further, decreased immunohistochemical staining for phospho-Rb was observed in tumors from mice treated with RRD-251 (Figure 4C, left panel). Quantification of the staining demonstrated a significantly decreased level of phospho-Rb in the tumor samples treated with RRD-251 (44.54±6.33% negative-weak, 5.23±2.49% strong) when compared to the control tumor samples (16.51±3.3% negative-weak, 51.17±6.29% strong (Figure 4C, right panel). To determine if RRD-251 affected the angiogenesis in the xenografted pancreatic cancers, tumors were stained for CD31 (Figure 4D, left panel). Supporting our *in vitro* results, tumors treated with RRD-251 demonstrated a

14-fold reduction in microvasculature (Figure 4D, right panel). These results suggest that inhibition of tumor growth by RRD-251 correlates with a disruption of the Rb-Raf-1 interaction, decrease in Rb phosphorylation, and angiogenesis.

An orthotopic model was used to investigate whether RRD-251 could prevent the metastasis of pancreatic tumors. Metastatic L3.6pl pancreatic cancer cells were implanted in the pancreas of nude mice; after 1-week of inoculation the mice were randomized into two groups and treated as described above. After 3-weeks of treatment, mice were euthanized and primary tumor growth in pancreas and metastasis to liver and lymph nodes was analyzed. RRD-251 significantly reduced primary tumor size (Figure 5A) and also significantly affected the tumors ability to metastasize to lymph nodes and liver as represented by H&E (Figure 5B). Tumor volume was reduced by approximately 90% and lymph node and liver metastases reduced by 83% and 100% respectively in mice treated with RRD-251. Additionally, Rb phosphorylation (p-Rb) was significantly higher at metastatic tumor sites compared to adjacent normal tissues (Figure 5C), suggesting Rb inactivation contributes to metastatic potential.

RRD-251 enhances the ability of gemcitabine to inhibit primary tumor growth

Attempts were next made to determine if RRD-251 could improve the effects of gemcitabine and inhibit the growth of gemcitabine resistant cells *in vivo*. A subcutaneous xenograft model utilizing the gemcitabine-sensitive L3.6pl and resistant L3.6pl^{GemRes} was utilized for this purpose. L3.6pl and L3.6pl^{GemRes} were implanted in the left and right flanks respectively. After tumors grew in each flank to approximately 100mm³, gemcitabine (250mg/kg, three times/week), RRD-251 (50mpk/daily), combination of gemcitabine and RRD-251, or DMSO/PBS vehicle were administered intraperitoneal. Tumors were measured every 2-4 days. After 16 days of treatment, the tumors were harvested. While gemcitabine significantly inhibited primary tumor growth in the gemcitabine-sensitive L3.6pl cells (Figure 6A), L3.6pl^{GemRes} tumor growth was heightened by gemcitabine (Figure 6B). RRD-251 alone significantly affected the growth of tumor growth regardless of chemosensitivity; in addition, combinations of RRD-251 with gemcitabine resulted in further tumor regression and almost complete tumor abrogation in both gemcitabine sensitive and resistant tumors (Figures 6C, 6D). These results suggest that combining RRD-251 with gemcitabine could be an effective therapy against pancreatic cancer.

Discussion

Although Rb itself has demonstrated mutations in various malignancies, the majority of tumors harbor mutations upstream of Rb, such as *K-Ras*, which is mutated in over 80% of PDAC (24). Specifically, a point mutation in codon 12 of the *K-Ras* oncogene in pancreatic adenocarcinoma leads to constitutive activation of downstream signal pathways, including the Raf-MEK-ERK and PI3-kinase cascades (25). While many attempts have been made to target the activation of Ras by using agents that prevent Ras prenylation, such methods have had limited success in the clinic.(26). Similarly, while the known downstream signaling pathways from *K-Ras* present promising avenues for drug development, such agents have had a minor impact on the control of pancreatic cancer (27). These results suggest downstream signaling cascades from Ras might not proceed in a linear fashion and components of this cascade might target various different substrates (28). Evidence suggests that binding of Raf-1 kinase activity to Raf-1 kinase inhibitor protein (RKIP), interrupts further downstream signaling (29) and potentially prevents inactivation of Rb resulting in tumor suppression. Therefore, it is not that surprising that increased Raf-1 kinase activity by loss of RKIP expression was associated with increased nodal and distant metastases in pancreatic ductal adenocarcinoma specimens and was independent predictor of worsening

disease-free survival of pancreatic ductal adenocarcinoma patients (30). Indeed, elevated levels of Raf-1 have been associated with Rb in non-small cell lung cancer samples compared to adjacent normal tissues, suggesting that this interaction might contribute to the oncogenic process (31). In our studies, when well and moderately differentiated tumors were compared to poorly and undifferentiated pancreatic adenocarcinomas, decreased differentiation of resected tumors correlated with increased levels of phospho-Rb. Additionally, investigations into clinical outcomes demonstrated reduced overall survival with reduced tumor differentiation and suggesting that more aggressive, undifferentiated tumors have more phosphorylated, inactive Rb. Although these data are correlative, further studies would be required to confirm the relationship between phosphorylation of Rb and clinical factors that affect overall patient outcomes. Our data demonstrate that specific disruption of Rb-Raf-1 interaction results in G1 cell-cycle arrest, induction of senescence, and significant inhibition of proliferation. We propose that these events are primarily due to the maintained binding of Rb to E2F family of transcription factors (32, 33), affecting the expression of genes involved in cell proliferation, senescence and apoptosis. As our results demonstrate, RRD-251 has not been found to affect the binding of E2F1 to Rb. We propose that the dissociation of Brg1 from Rb, since Rb remains hypophosphorylated. Therefore, it is likely that Rb phosphorylation, which has been established as a cellular target of the Raf-1 kinase, could be a suitable target for pancreatic adenocarcinoma. Our present studies demonstrate that disruption of the Rb-Raf-1 kinase interaction affects Rb phosphorylation and the malignant properties of pancreatic adenocarcinoma cells.

Similar to previous reports in melanoma (7), exposure of RRD-251 resulted in apoptosis of pancreatic cancer cell lines by affecting the levels of anti-apoptotic Bcl-2 and Mcl-1 and pro-apoptotic Bax proteins. These inhibitory effects of RRD-251 with gemcitabine were also observed in anchorage-independent cell growth, migration, and invasion, which are key features for carcinogenesis and malignant transformation. The clinical challenge in management of pancreatic cancer with aggressive phenotypes that result in early metastases is the resistance to the current first line chemotherapeutic agent, gemcitabine. In most preclinical models of pancreatic cancer, gemcitabine chemotherapy results in suppression of cell growth and apoptosis. Unfortunately, the continued use of gemcitabine can result in the development of chemotherapy resistance and overexpression of a variety of survival mechanisms, including the activation of the Akt/mTOR pathway. Recent evidence supports gemcitabine activation of a variety of proliferative and anti-apoptotic pathways in cancer cells (34). G2/M cell-cycle arrest with cyclin-dependent kinase inhibitors has been demonstrated to induce senescence (22, 23) and also inhibit pro-apoptotic pathways that might contribute to chemoresistance (35). Our studies show that while L3.6pl and L3.6pl^{GemRes} resist the apoptotic effects of RRD-251, this therapy induces senescence. An apoptotic effect was observed when combined with gemcitabine in L3.6pl^{GemRes}, with a re-establishment of sensitivity to gemcitabine observed in the parental L3.6pl cells. It is conceivable that induction of senescence with RRD-251 might inhibit pro-apoptotic pathways, such as Akt-mTOR, and restore sensitivity in otherwise chemoresistant phenotypes. We also propose that anti-tumor effects of RRD-251 were exerted in partly limiting angiogenesis. This is supported by the studies showing that Raf-1 kinase contributes to angiogenesis (36, 37); this might involve inactivation of Rb with subsequent induction of E2F-1 mediated FLT-1 and KDR transcriptional activation.

Identification of RRD-251 as a selective inhibitor of Rb-Raf-1 interaction is an example of targeting protein-protein interactions for pancreatic cancer therapy. In this study, we demonstrate the importance of a small molecule that can maintain the tumor suppressor function of Rb by disrupting its physical interaction with other proteins and also enhance the effects of gemcitabine chemotherapy. We believe these discoveries will ultimately lead to new therapeutic strategies to combat cancer.

Supplementary Material

Refer to Web version on PubMed Central for supplementary material.

Acknowledgments

Support of the Core Facilities at Moffitt Cancer Center is greatly appreciated.

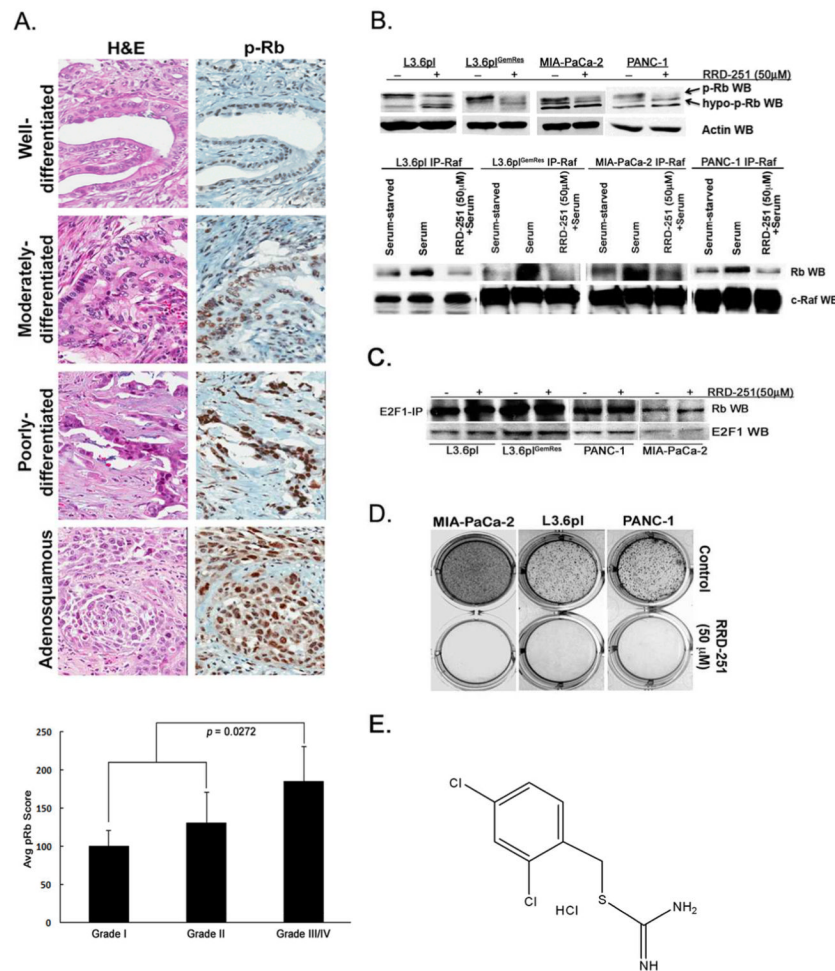
Grant Support: This study was supported by the NCI Grant 1PO1CA118210 to S. Sebti; Project 4 supported S. Chellappan and these studies.

References

1. Siegel R, Naishadham D, Jemal A. Cancer statistics, 2012. *CA Cancer J Clin.* 2012; 62:10–29. [PubMed: 22237781]
2. Hidalgo M. Pancreatic cancer. *N Engl J Med.* 2010; 362:1605–17. [PubMed: 20427809]
3. Haggmann W, Jesnowski R, Lohr JM. Interdependence of gemcitabine treatment, transporter expression, and resistance in human pancreatic carcinoma cells. *Neoplasia.* 2010; 12:740–7. [PubMed: 20824050]
4. Wang Z, Li Y, Kong D, Banerjee S, Ahmad A, Azmi AS, et al. Acquisition of epithelial-mesenchymal transition phenotype of gemcitabine-resistant pancreatic cancer cells is linked with activation of the notch signaling pathway. *Cancer Res.* 2009; 69:2400–7. [PubMed: 19276344]
5. Davis RK, Chellappan S. Disrupting the Rb-Raf-1 interaction: a potential therapeutic target for cancer. *Drug News Perspect.* 2008; 21:331–5. [PubMed: 18836591]
6. Johnson JL, Pillai S, Pernazza D, Sebti SM, Lawrence NJ, Chellappan SP. Regulation of matrix metalloproteinase genes by E2F transcription factors: Rb-Raf-1 interaction as a novel target for metastatic disease. *Cancer Res.* 2012; 72:516–26. [PubMed: 22086850]
7. Singh S, Davis R, Alamanda V, Pireddu R, Pernazza D, Sebti S, et al. Rb-Raf-1 interaction disruptor RRD-251 induces apoptosis in metastatic melanoma cells and synergizes with dacarbazine. *Mol Cancer Ther.* 2010; 9:3330–41. [PubMed: 21139044]
8. Chellappan SP, Hiebert S, Mudryj M, Horowitz JM, Nevins JR. The E2F transcription factor is a cellular target for the RB protein. *Cell.* 1991; 65:1053–61. [PubMed: 1828392]
9. Wang S, Ghosh RN, Chellappan SP. Raf-1 physically interacts with Rb and regulates its function: a link between mitogenic signaling and cell cycle regulation. *Mol Cell Biol.* 1998; 18:7487–98. [PubMed: 9819434]
10. Dasgupta P, Sun J, Wang S, Fusaro G, Betts V, Padmanabhan J, et al. Disruption of the Rb-Raf-1 interaction inhibits tumor growth and angiogenesis. *Mol Cell Biol.* 2004; 24:9527–41. [PubMed: 15485920]
11. Kinkade R, Dasgupta P, Carie A, Pernazza D, Carless M, Pillai S, et al. A small molecule disruptor of Rb/Raf-1 interaction inhibits cell proliferation, angiogenesis, and growth of human tumor xenografts in nude mice. *Cancer Res.* 2008; 68:3810–8. [PubMed: 18483265]
12. Hashimoto K, Nio Y, Koike M, Itakura M, Yano S, Higami T, et al. Expression of retinoblastoma and p53 pathway-related proteins in resectable invasive ductal carcinoma of the pancreas: potential cooperative effects on clinical outcome. *Anticancer Res.* 2005; 25:1361–8. [PubMed: 15865092]
13. Yuan LW, Tang W, Kokudo N, Seyama Y, Shi YZ, Karako H, et al. Disruption of pRb-p16INK4 pathway: a common event in ampullary carcinogenesis. *Hepatogastroenterology.* 2005; 52:55–9. [PubMed: 15782994]
14. Bruns CJ, Harbison MT, Kuniyasu H, Eue I, Fidler IJ. In vivo selection and characterization of metastatic variants from human pancreatic adenocarcinoma by using orthotopic implantation in nude mice. *Neoplasia.* 1999; 1:50–62. [PubMed: 10935470]
15. Trevino JG, Summy JM, Gray MJ, Nilsson MB, Lesslie DP, Baker CH, et al. Expression and activity of SRC regulate interleukin-8 expression in pancreatic adenocarcinoma cells: implications for angiogenesis. *Cancer Res.* 2005; 65:7214–22. [PubMed: 16103072]

16. Duxbury MS, Ito H, Zinner MJ, Ashley SW, Whang EE. Inhibition of SRC tyrosine kinase impairs inherent and acquired gemcitabine resistance in human pancreatic adenocarcinoma cells. *Clin Cancer Res.* 2004; 10:2307–18. [PubMed: 15073106]
17. Vindelov LL, Christensen IJ, Keiding N, Spang-Thomsen M, Nissen NI. Long-term storage of samples for flow cytometric DNA analysis. *Cytometry.* 1983; 3:317–22. [PubMed: 6839880]
18. Vermes I, Haanen C, Steffens-Nakken H, Reutelingsperger C. A novel assay for apoptosis. Flow cytometric detection of phosphatidylserine expression on early apoptotic cells using fluorescein labelled Annexin V. *J Immunol Methods.* 1995; 184:39–51. [PubMed: 7622868]
19. Trevino JG, Summy JM, Lesslie DP, Parikh NU, Hong DS, Lee FY, et al. Inhibition of SRC expression and activity inhibits tumor progression and metastasis of human pancreatic adenocarcinoma cells in an orthotopic nude mouse model. *Am J Pathol.* 2006; 168:962–72. [PubMed: 16507911]
20. Pillai S, Kovacs M, Chellappan S. Regulation of vascular endothelial growth factor receptors by Rb and E2F1: role of acetylation. *Cancer Res.* 2010; 70:4931–40. [PubMed: 20516113]
21. Tubbs RR, Pettay J, Barry TS, Swain E, Loftus M, Cook JR, et al. The specificity of interphase FISH translocation probes in formalin fixed paraffin embedded tissue sections is readily assessed using automated staining and scoring of tissue microarrays constructed from murine xenografts. *J Mol Histol.* 2007; 38:159–65. [PubMed: 17094016]
22. Capparelli C, Chiavarina B, Whitaker-Menezes D, Pestell TG, Pestell RG, Hult J, et al. CDK inhibitors (p16/p19/p21) induce senescence and autophagy in cancer-associated fibroblasts, "fueling" tumor growth via paracrine interactions, without an increase in neo-angiogenesis. *Cell Cycle.* 2012; 11:3599–610. [PubMed: 22935696]
23. Michaud K, Solomon DA, Oermann E, Kim JS, Zhong WZ, Prados MD, et al. Pharmacologic inhibition of cyclin-dependent kinases 4 and 6 arrests the growth of glioblastoma multiforme intracranial xenografts. *Cancer Res.* 2010; 70:3228–38. [PubMed: 20354191]
24. Almoguera C, Shibata D, Forrester K, Martin J, Arnheim N, Perucho M. Most human carcinomas of the exocrine pancreas contain mutant c-K-ras genes. *Cell.* 1988; 53:549–54. [PubMed: 2453289]
25. Campbell SL, Khosravi-Far R, Rossman KL, Clark GJ, Der CJ. Increasing complexity of Ras signaling. *Oncogene.* 1998; 17:1395–413. [PubMed: 9779987]
26. Berndt N, Hamilton AD, Sebt SM. Targeting protein prenylation for cancer therapy. *Nat Rev Cancer.* 2011; 11:775–91. [PubMed: 22020205]
27. Rinehart J, Adjei AA, Lorusso PM, Waterhouse D, Hecht JR, Natale RB, et al. Multicenter phase II study of the oral MEK inhibitor, CI-1040, in patients with advanced non-small-cell lung, breast, colon, and pancreatic cancer. *J Clin Oncol.* 2004; 22:4456–62. [PubMed: 15483017]
28. Kindler HL, Wroblewski K, Wallace JA, Hall MJ, Locker G, Nattam S, et al. Gemcitabine plus sorafenib in patients with advanced pancreatic cancer: a phase II trial of the University of Chicago Phase II Consortium. *Invest New Drugs.* 2012; 30:382–6. [PubMed: 20803052]
29. Yeung K, Janosch P, McFerran B, Rose DW, Mischak H, Sedivy JM, et al. Mechanism of suppression of the Raf/MEK/extracellular signal-regulated kinase pathway by the raf kinase inhibitor protein. *Mol Cell Biol.* 2000; 20:3079–85. [PubMed: 10757792]
30. Kim HS, Kim GY, Lim SJ, Kim YW. Loss of Raf-1 kinase inhibitory protein in pancreatic ductal adenocarcinoma. *Pathology.* 2010; 42:655–60. [PubMed: 21080875]
31. Dasgupta P, Kinkade R, Joshi B, Decook C, Haura E, Chellappan S. Nicotine inhibits apoptosis induced by chemotherapeutic drugs by up-regulating XIAP and survivin. *Proc Natl Acad Sci U S A.* 2006; 103:6332–7. [PubMed: 16601104]
32. Chen T, Xue L, Niu J, Ma L, Li N, Cao X, et al. The Retinoblastoma Protein Selectively Represses E2F1 Targets via a TAAC DNA Element during Cellular Senescence. *J Biol Chem.* 2012; 287:37540–51. [PubMed: 22955272]
33. Harbour JW, Dean DC. Rb function in cell-cycle regulation and apoptosis. *Nat Cell Biol.*
34. Adesso L, Calabretta S, Barbagallo F, Capurso G, Pillozzi E, Geremia R, et al. Gemcitabine triggers a pro-survival response in pancreatic cancer cells through activation of the MNK2/eIF4E pathway. *Oncogene.*

35. Subramaniam D, Periyasamy G, Ponnurangam S, Chakrabarti D, Sugumar A, Padigar M, et al. CDK-4 inhibitor P276 sensitizes pancreatic cancer cells to gemcitabine-induced apoptosis. *Mol Cancer Ther.* 2012; 11:1598–608. [PubMed: 22532602]
36. Hood JD, Cheres DA. Targeted delivery of mutant Raf kinase to neovessels causes tumor regression. *Cold Spring Harb Symp Quant Biol.* 2002; 67:285–91. [PubMed: 12858551]
37. Suzuma K, Takahara N, Suzuma I, Isshiki K, Ueki K, Leitges M, et al. Characterization of protein kinase C beta isoform's action on retinoblastoma protein phosphorylation, vascular endothelial growth factor-induced endothelial cell proliferation, and retinal neovascularization. *Proc Natl Acad Sci U S A.* 2002; 99:721–6. [PubMed: 11805327]



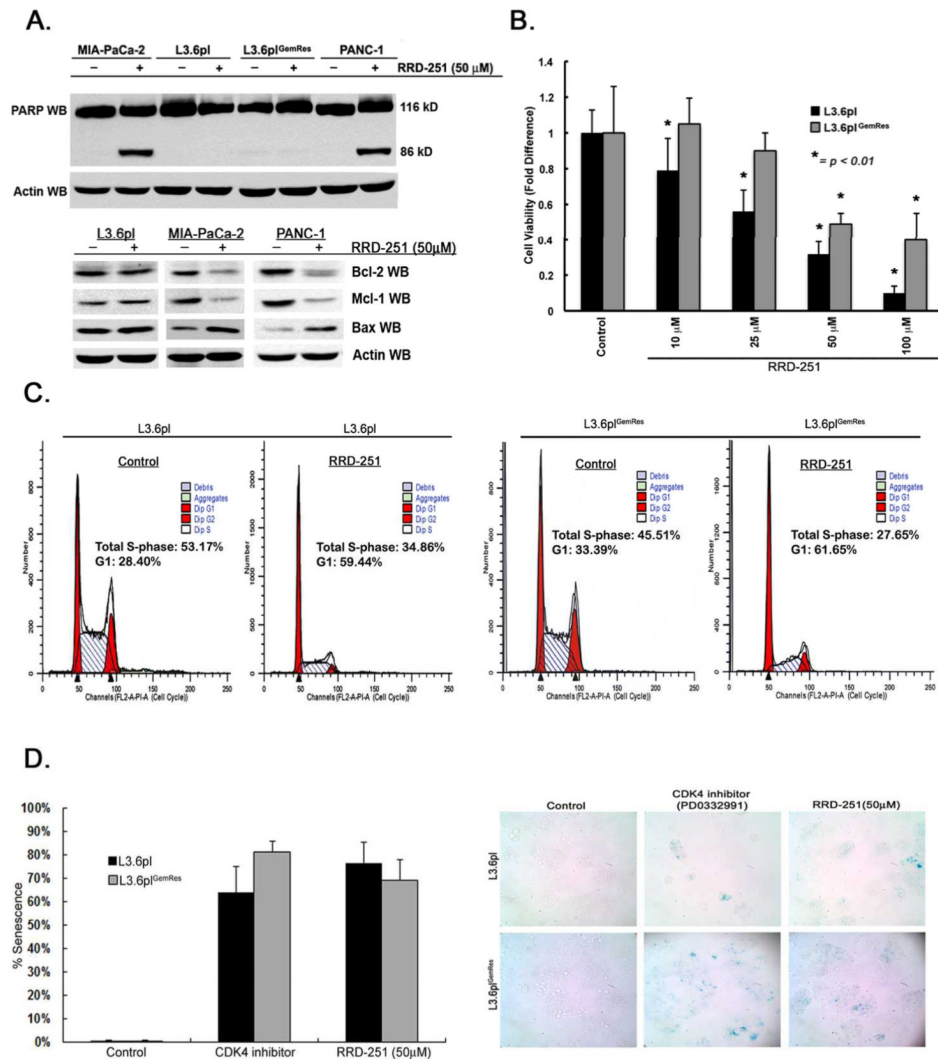


Figure 2. Disruption of Rb-Raf-1 kinase interactions with RRD-251 induces cell-cycle arrest, inhibit proliferation, and induce senescence in metastatic/chemoresistant pancreatic cancer variants. A, Pancreatic cancer cells treated with RRD-251 show PARP cleavage, along with a decrease in anti-apoptotic proteins Bcl-2, Mcl-1 and increase in pro-apoptotic protein Bax (lower panel). B, RRD-251 significantly affects cell proliferation/viability in a dose-dependent manner on L3.6pl and L3.6pl^{GemRes} metastatic pancreatic cancer cells ($p < 0.01$). C, Cell-cycle analysis demonstrates a significant arrest in S-phase entry in metastatic (left panels) and gemcitabine-resistant variants treated with RRD-251 (right panels). D, Measured (left panel) and representative images (right panel) of senescence in L3.6pl and L3.6pl^{GemRes} metastatic pancreatic cancer cells treated with RRD-251 comparable to positive control CDK4 inhibitor PD0332991.

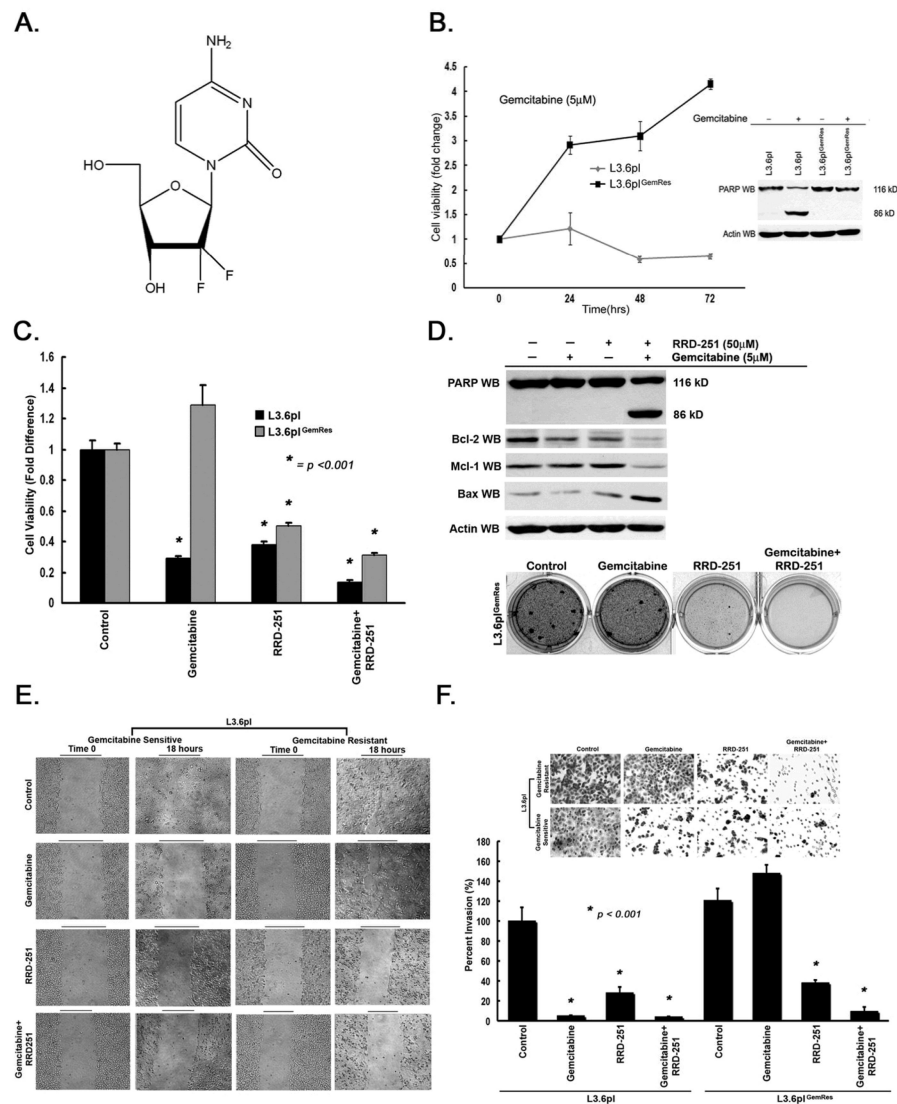


Figure 3. RRD-251 enhances the effects of gemcitabine. **A**, Chemical structure of gemcitabine. **B**, Gemcitabine has no effect on L3.6pl^{GemRes} cell proliferation and do not demonstrate PARP cleavage in the presence of gemcitabine when compared to parental gemcitabine-sensitive L3.6pl. **C**, L3.6pl and L3.6pl^{GemRes} pancreatic cancer cells treated with RRD-251 demonstrated a significant decrease in cell viability/proliferation with a augmented inhibitory effect noted with gemcitabine combination (**p* < 0.001). **D**, L3.6pl^{GemRes} cells treated with combination RRD-251 and gemcitabine demonstrated robust PARP cleavage (upper panel). There was a decrease in anti-apoptotic proteins Bcl-2, Mcl-1 and increase in pro-apoptotic protein Bax (middle panel). RRD-251 significantly inhibits anchorage-independent growth of L3.6pl^{GemRes} cells and enhances the effects of gemcitabine chemotherapy (lower panel). RRD-251 significantly inhibited the migratory (**E**) and invasive (**F**, qualitative upper panel, quantitative lower panel) ability of metastatic variant L3.6pl and gemcitabine-resistant L3.6pl^{GemRes} while demonstrating further inhibition of invasion with the addition of gemcitabine (*p* < 0.001).

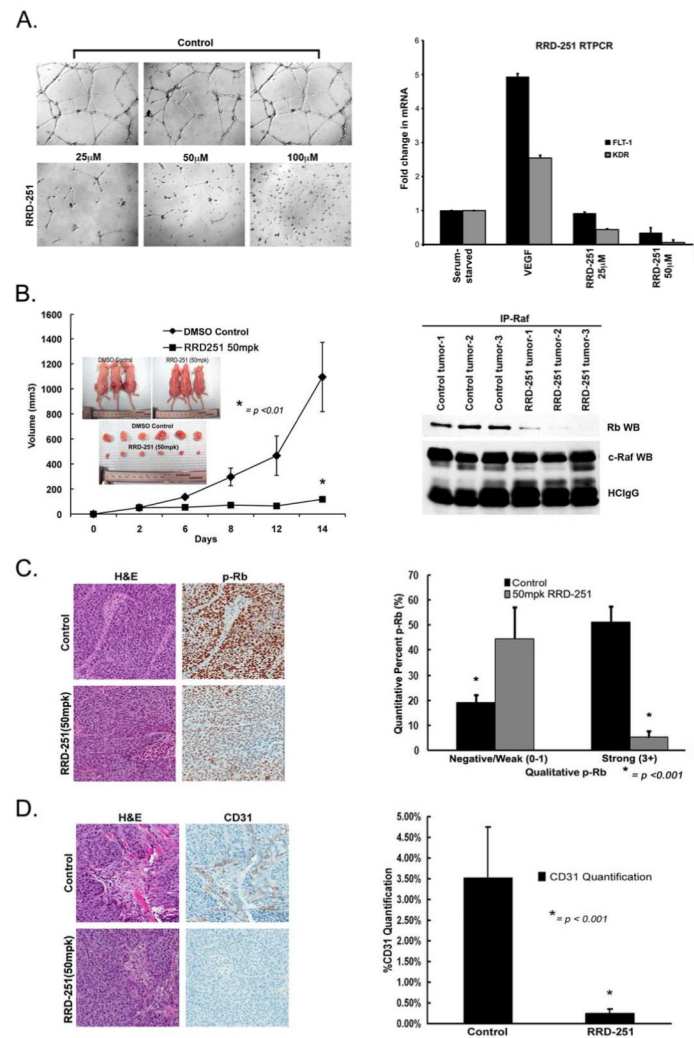


Figure 4. RRD-251 inhibits primary tumor growth in a subcutaneous tumor model by decreasing angiogenic potential. A, Interruption of capillary tube formation of HUVEC cells was observed with RRD-251 treatment in a matrigel angiogenesis tubule formation assay (left panel) and RRD-251 inhibited vascular endothelial growth factor (VEGF) induction of FLT-1 and KDR mRNA (right panel). B (left panel), Mice treated with RRD-251 showed tumor growth inhibition when compared to DMSO control ($*p < 0.01$). B (inlet), Size differences were evident *in vivo* and *ex vivo*. B (right panel), Disruption of the Rb-Raf-1 interaction by RRD-251 in the tumor lysates was observed in an immunoprecipitation-western blot experiment. C, Immunohistochemical analysis of tumor samples demonstrated a significant reduction in Rb phosphorylation in RRD-251 treated mice (left panel). Results were quantified in each group and represented as negative-weak and strong expression ($*p < 0.01$) (right panel). D, CD31 staining demonstrated an inhibitory effect of RRD-251 on angiogenesis *in vivo* (left panel). CD31 quantification was performed on tumor samples of mice treated with RRD-251 and control as previously described ($*p < 0.001$) (right panel).

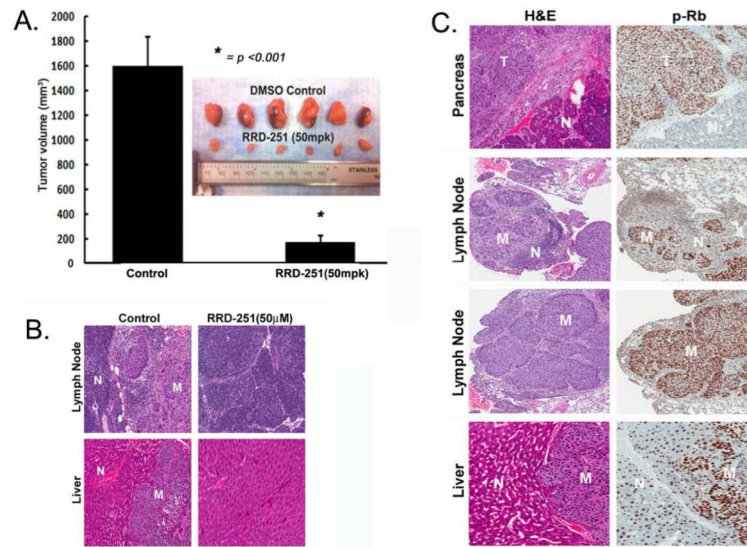


Figure 5. RRD-251 inhibits orthotopic tumor growth and metastasis. A, Mice treated with RRD-251 had a significant decrease in primary orthotopic tumor growth ($*p < 0.01$). B, Representative H&E tumor samples (T) of mice treated with RRD-251 demonstrates the loss of metastases (M) to liver and lymph nodes adjacent to normal tissue (N). C, Expression levels of phospho-Rb (p-Rb) are higher in lymph node and liver metastatic sites (M) of control mice when compared to the unaffected lymph node and liver tissue (N) of mice treated with RRD-251.

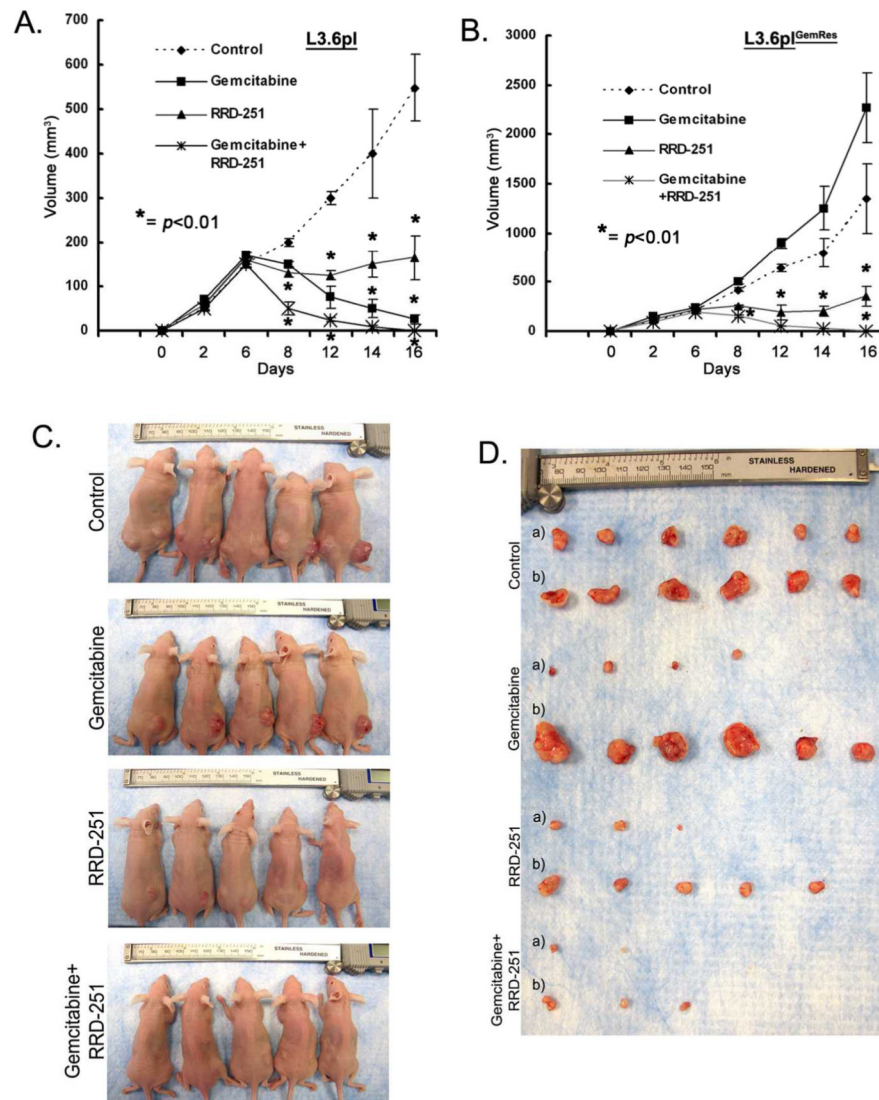


Figure 6. RRD-251 enhances the effects of gemcitabine to inhibit tumor growth. A, B, While gemcitabine-resistant variant L3.6pl^{GemRes} continue to grow in the presence of gemcitabine, growth was significantly inhibited in the RRD-251 group and abrogated with combination therapy ($*p < 0.01$). In L3.6pl cells, gemcitabine resulted in regression of disease, RRD-251 stabilized growth, and combination therapy almost completely abolished tumor growth ($*p < 0.01$). C, D, Tumors *in vivo* (L3.6pl, left flank and L3.6pl^{GemRes}, right flank) and *ex vivo* {L3.6pl, a) and L3.6pl^{GemRes}, b)} demonstrating the differences in tumor size of the L3.6pl^{GemRes} {right flank, b)} in the presence of gemcitabine and also the significant inhibitory effect of RRD-251 alone and in combination with gemcitabine on both tumors regardless of gemcitabine sensitivity.